

Shannon Entropy Analysis of Reservoir-Triggered Seismicity at Song Tranh 2 Hydropower Plant, Vietnam

Luciano Telesca ^{1,*} , Anh Tuan Thai ², Michele Lovallo ³, Dinh Trong Cao ² and Le Minh Nguyen ²

¹ Institute of Methodologies for Environmental Analysis, National Research Council, C. da S. Loja, 85050 Tito, Italy

² Institute of Geophysics, Vietnam Academy of Science and Technology, Hanoi 100000, Vietnam

³ Agenzia Regionale per la Protezione dell'Ambiente della Basilicata (ARPAB), 85100 Potenza, Italy

* Correspondence: luciano.telesca@imaa.cnr.it

Abstract: The reservoir-triggered seismicity at the Song Tranh 2 reservoir in Vietnam is investigated by using Shannon entropy, a well-known informational method used to analyze complexity in time series in terms of disorder and uncertainty. The application of the time-varying Shannon entropy to the time series of the interevent times of seismicity has evidenced clear links with the temporal fluctuations of the water level of the reservoir, strengthening the belief that the reservoir operational regime is one of the sources of the seismicity occurring in the area. Shannon entropy has also shed light on the tectonic mechanisms of generation of reservoir-triggered seismicity, revealing that the change in stress due to the variation in water level causes the seismic system to be in a state of greater disorder and instability, well depicted by Shannon entropy, which would lead to an increase in seismic activity.

Keywords: Shannon entropy; earthquakes; reservoir-triggered seismicity



Citation: Telesca, L.; Thai, A.T.; Lovallo, M.; Cao, D.T.; Nguyen, L.M. Shannon Entropy Analysis of Reservoir-Triggered Seismicity at Song Tranh 2 Hydropower Plant, Vietnam. *Appl. Sci.* **2022**, *12*, 8873. <https://doi.org/10.3390/app12178873>

Academic Editors: Melvin M. Vopson and Jaewoo Joo

Received: 1 July 2022

Accepted: 1 September 2022

Published: 4 September 2022

Publisher's Note: MDPI stays neutral with regard to jurisdictional claims in published maps and institutional affiliations.



Copyright: © 2022 by the authors. Licensee MDPI, Basel, Switzerland. This article is an open access article distributed under the terms and conditions of the Creative Commons Attribution (CC BY) license (<https://creativecommons.org/licenses/by/4.0/>).

1. Introduction

Reservoir-triggered seismicity (RTS) has been the subject of many scientific papers in recent times due to its ability to cause damage to buildings and infrastructure and, in the worst case, to kill people. The main cause of RTS is additional static loading due to the weight of water reservoirs, tectonic faults, liquefaction, and variations in pore pressure. Several studies of RTS have been carried out worldwide [1–7], and all of them reached the same conclusion that reservoir-filling influences the seismic regime of areas with active tectonic faults. The operational regime of a dam is generally oscillating and driven by the seasonal cycle of the water level [3]. Pore fluid pressure diffusion underneath the reservoir or the gravitational loading of the reservoir [8–10] are considered the main mechanisms of RTS. Mikhailov et al. [5] proposed that seismic events are triggered by “ambient stress field conditions (as a result of the water load which may lead to a failure), fracture occurrence, hydromechanical properties of the rocks beneath the reservoir, geology of the area, dimensions of the reservoir and lake-level fluctuation.” Rajendran et al. [11] suggested that RTS originates in the violation of equilibrium due to the “reduction in the strength of the fault zones.” This finding was later refined in Rajendran and Harish [1], who concluded that “water passes through the basalts broken by the meridional faults and penetrates into the fault zone with the highly permeable” layers. There have been several cases reported worldwide where earthquakes, even large ones, occurred years after the impoundment of the reservoir in areas that were practically aseismic before the impoundment [12].

Among the various ways to characterize the dynamics of a time series is the amount or degree of uncertainty or disorder; this is quantified by Shannon entropy (SE), which is large for very disordered series and low for very organized ones.

SE has found successful application in the investigation of various complex nonstationary time series [13] and, in particular, in the study of the dynamics of earthquakes. Previous studies investigated the relationship between the SE and the progressive failure processes of the rocks leading to earthquakes, greatly depending on the heterogeneities of the crust [14]. Guarino et al. [15] analyzed the pattern of the microfractures occurring before the final crack on heterogeneous materials by recording the acoustic emissions under progressive load; they found a decrease in the SE. Lu et al. [16] found that SE decreases before a large event by investigating the micro-seismicity preceding a rock burst in a galena mine. Similar results were discussed in Chelidze et al. [17] in connection with the magnitude series of large Caucasian earthquakes. Recently, Rundle et al. [18] applied the concept of SE to seismic nowcasting. In this context, in our study we perform an entropic analysis of seismicity triggered by the Song Tranh 2 reservoir by using SE, which, to our knowledge, has not been used to investigate the time dynamics of reservoir-triggered seismicity so far.

2. Seismotectonic Settings and Data

The central part of the Vietnamese continental margin forms the transition from the continental Indochina Block to the East Sea (or South China Sea), which makes the margin a key area for understanding the complex Cenozoic development of Indochina and the East Sea [19–21]. The Song Tranh 2 reservoir is located on the metamorphic rocks of the Tra Bong and Kham Duc complex formations [22,23]. The original rock in the study region is primarily metamorphic amphibolite, formed during the orogenic movement of Indochina, which occurred about 245–250 million years ago. Research shows that the study region and its vicinity have undergone several stages of tectonic movements with different distortional characteristics. There were two main ductile deformational phases with the general movement mechanism slipping, including: early phase axis, compressive strain axis, and sub-latitude. Under this stress field, the NW-SE fracture activity slid to the left; by contrast, distortion in the later phase featured local compressive axial sub-meridian and enjoyed the strain axes of the sub-latitude. Under the action of this stress field, the NW-SE fracture slid right. The Cenozoic tectonic motion of the later phase had close ties with volcanic activities in central and southern Vietnam during the Neogene-Quaternary. The Song Tranh 2 reservoir is located within a series of zones with split-snowboarding by NW-SE direction, which tended to raise the compression zone sub-meridian direction and which also creates an E-W spreading trend. The sub-latitude and the NE-SW directions faults are underdeveloped, while the sub-meridian direction fault is hardly absent. There are three main faults: Tra Bui–Tra Nu (F1), Phuoc Gia–Tra Kot (F8), and Tra Leng–Tra Khe (F12); all the remaining faults are branches of the main faults [22,23]. All the faults are very steep or vertical, striking NW-SE and exhibiting right–lateral strike slip motion (Figure 1).

The Song Tranh 2 region is a site of reservoir-triggered seismicity, where the seismic activity is controlled by the pore pressure and water level change due to the water impoundment [24]. The Song Tranh 2 hydropower reservoir was impounded in November 2010 and seismicity increased in 2011, with earthquakes continuing to occur. Every year several thousands of earthquakes occur, and there are no signs of decline. The largest earthquake, of ML 4.7, occurred on 15 November 2012, causing minor damage to houses in the Tra My district.

Digital data acquisition systems were deployed by the Institute of Geophysics (VAST) in the vicinity of the Song Tranh 2 reservoir to get a large amount of data and to help in understanding the physical processes responsible for generating earthquakes in the area.

A seismic network of 10 stations was established by the Institute of Geophysics–Vietnam Academy of Science and Technology (IGP-VAST). The stations are installed on the hard rock site and the distance from the epicenters to 10 stations ranges from 4 to 23 km. These stations were equipped with Guralp CMG-6TD seismometers. Guralp seismometers have on-board digitizers with a dynamic range of 130 dB. During the observation period of September 2012 to March 2020, about 8,000 earthquakes were reported by IGP-VAST. These earthquake epicenters are shown in Figure 1.

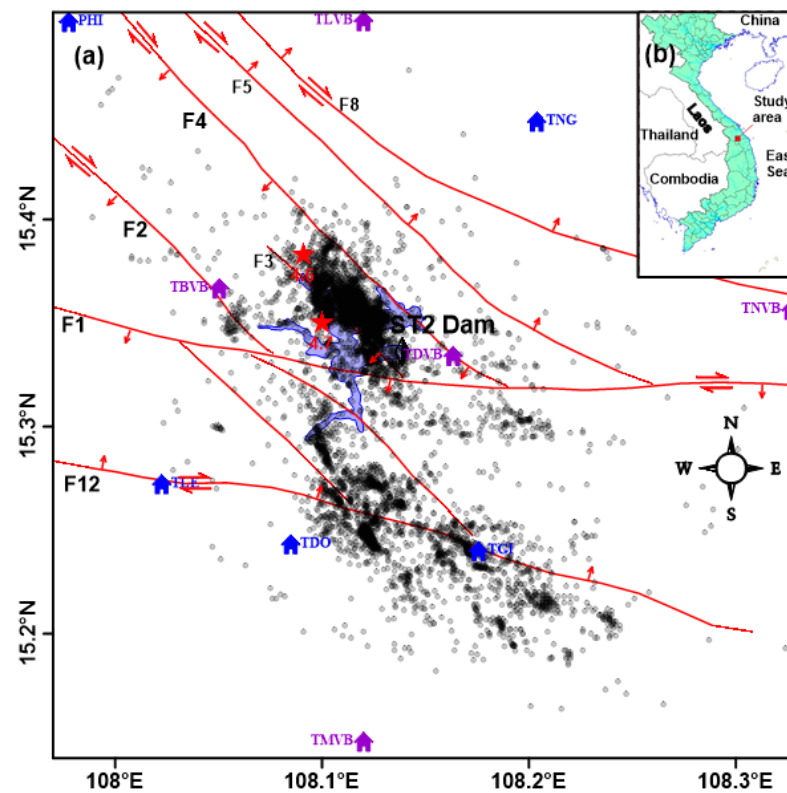


Figure 1. (a) Spatial distribution of earthquake epicenters during the period of September 2012 to March 2020 (dark circles) near the Song Tranh 2 reservoir (light blue). The investigation area, represented by the red square in the inner map (b), is located in the center of Vietnam. The earthquakes with ML 4.7 and 4.6 are indicated by red stars. Geology and identified geologically mapped faults (red) with dip and slip direction as given by Hoai et al. [22,23].

3. Shannon Entropy

Shannon entropy (SE) furnishes a characterization of the probability density function of a series on a global scale [25] and can be used to analyze the complexity of nonstationary time series in terms of disorder or uncertainty [26]. The SE is defined through the following formula:

$$SE = - \int_{-\infty}^{+\infty} f_X(x) \log f_X(x) dx, \tag{1}$$

where $f(x)$ is the probability density function of the series x . As the calculation of SE depends on $f(x)$, this has to be accurately estimated. In this paper, the estimation of $f(x)$ was performed by applying the kernel-based approach, which has been shown to perform better than the discrete-based approach in calculating the SE for Gaussian processes [27]. The kernel-based approach is based on the kernel density estimator technique [28,29]:

$$\hat{f}_M(x) = \frac{1}{Mb} \sum_{i=1}^M K\left(\frac{x - x_i}{b}\right), \tag{2}$$

where $\hat{f}_M(x)$ is the estimate of $f(x)$, b refers to the bandwidth, M represents the number of data, and $K(u)$ is a continuous non-negative and symmetric kernel function that satisfies the following two conditions:

$$K(u) \geq 0 \text{ and } \int_{-\infty}^{+\infty} K(u) du = 1, \tag{3}$$

The estimation of $f(x)$ uses an optimized integrated method that combines the algorithms of Troudi et al. [30] and Raykar and Duraiswami [31]; the method consists in finding the optimal value of the bandwidth b [27] for the kernel estimation of $f(x)$. In particular, by using a zero mean and unit variance Gaussian kernel, the estimate of $f(x)$ is the following:

$$\hat{f}_M(x) = \frac{1}{M\sqrt{2\pi}b^2} \sum_{i=1}^M e^{-\frac{(x-x_i)^2}{2b^2}}. \quad (4)$$

4. Results

In this study we analyzed the series of interevent times $\Delta\tau$, which is the series of time intervals between two consecutive events. Based on the results by Telesca et al. [32], the completeness magnitude of the analyzed seismic catalogue is 1.7; thus, the series was computed considering only events with a magnitude larger or equal to 1.7.

According to Vogel et al. [33], in this study we calculated the time varying SE by sliding a fixed-length window through the series. We set the length of the window at $N = 50$ and $N = 100$ data in order to check for dependence on the window length. In both cases, we shifted the window by one datum, associating the calculated value of SE to the time of occurrence of the last event in the window. This procedure guaranteed enough smoothing among the values and allowed us to evaluate their variation with a good resolution.

Figure 2 shows the results for the interevent times $\Delta\tau$. A clear variability characterizes the time pattern of SE, suggesting the changing dynamics of the seismic process between disordered states (high SE) and ordered states (low SE). The curves obtained with the two values of the window lengths are quite similar, suggesting the robustness of the results against the length of the moving window. Most strikingly, the spike-like behavior of the SE time pattern reflects the oscillatory behavior of the water level. In particular, most of the relative maxima of the SE occur within the annual cycle of the water level; the exception was during 2018–2019, in which the water level exhibited rather anomalous cyclic behavior characterized by three cycles (two large ones and a very small one in the middle). This anomalous water cyclic behavior probably “breaks” the correlative relationship between the SE and the water level, which is instead characterized by the coincidence of most of the relative maxima of the SE with the annual cycle of the water level. This indicates that the seismic process taking place at Song Tranh 2 reservoir changes its status with dynamic transitions that could be triggered by fluctuations in the water level. Figure 3 shows the comparison between the frequency of $\Delta\tau$ in two windows, where the SE is maximum (10 February 2017) and minimum (13 March 2018), respectively, for the whole catalogue with a moving window of length of $N = 100$. As can be seen, the frequency distribution of the interevent times in the window where SE is the minimum (black) is characterized by a more peaked behavior and smaller width than those featuring the frequency distribution in the window with the maximum SE (red). The modulating behavior of the SE reflects the modulating behavior of the time dynamics of the seismicity. The $\Delta\tau$ frequency distribution of the seismicity changes between more peaked and narrower to less peaked and wider shapes, which could reflect the changing tectonic stress status of the area subjected to the cyclic trend of the water level.

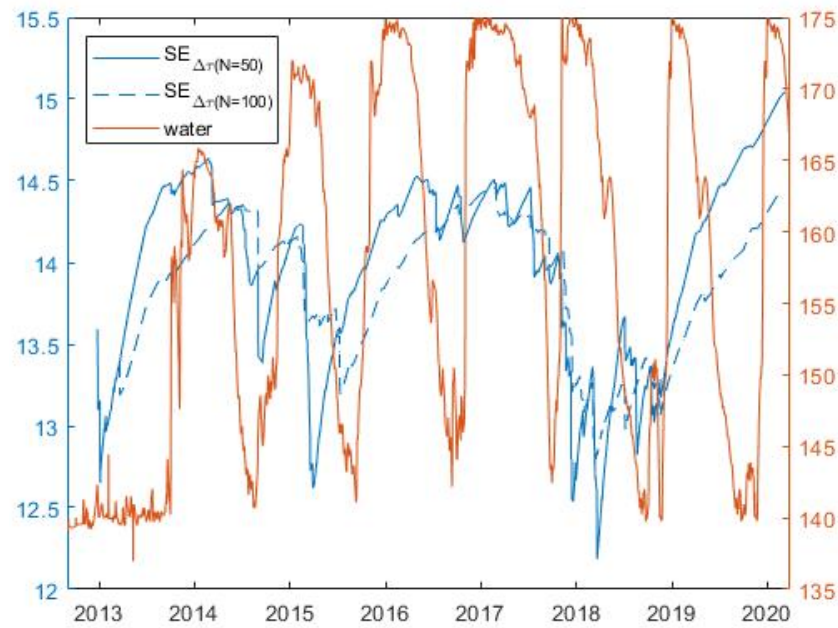


Figure 2. SE of $\Delta\tau$ for the whole seismic catalogue (blue) and water level (red). Two different lengths of moving windows have been selected for calculating SE: $N = 50$ (solid) and $N = 100$ (dashed).

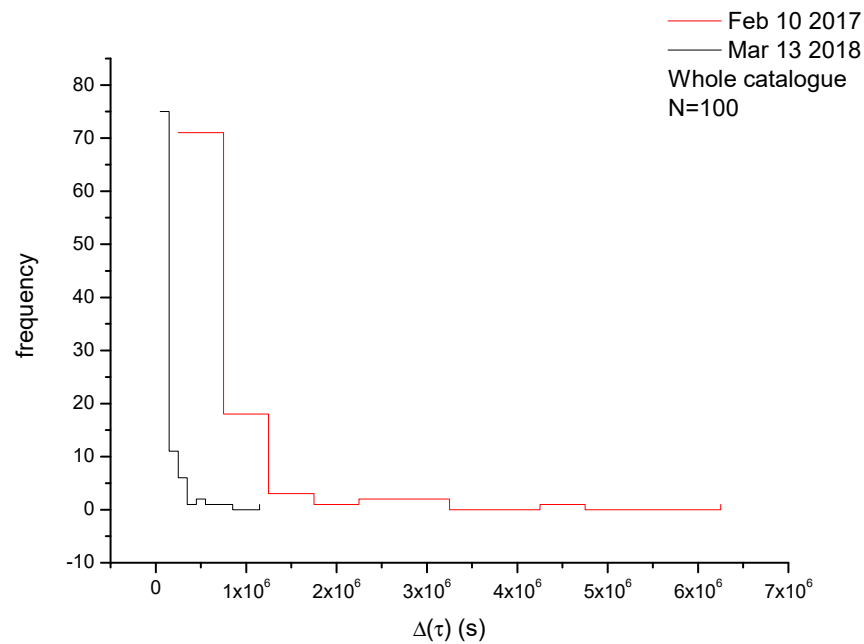


Figure 3. Comparison between frequency of $\Delta\tau$ in two different windows corresponding to maximum (red) and minimum (black) SE for the whole catalogue with a moving window of length $N = 100$.

Since the results could be influenced by the existence of possible clusters in the data, we de-clustered the seismic catalogue and applied time-varying Shannon entropy to the interevent times of the de-clustered catalogue. We de-clustered the seismic catalogue by means of the method developed by Zaliapin et al. [34] based on nearest-neighbor (NN) distance in the space–time–energy domain between events i and j [35]:

$$\eta_{ij} = \begin{cases} c\tau_{ij}r_{ij}^{d_f}10^{-\omega m_i} & \tau_{ij} > 0 \\ \infty & \tau_{ij} \leq 0 \end{cases} \quad (5)$$

where τ_{ij} is the time interval (in years) between events i and j (positive or negative, if earthquake i preceded or followed earthquake j), r_{ij} is their spatial distance (in km), d_f is the fractal dimension of the spatial distribution of the epicenters [34], and w is the parameter that introduces the exponential weight of the earlier event i by its magnitude [36]. We set w equal to 0 for de-clustering purposes [37]. If the seismicity is not clustered or Poissonian, the distribution of η_{ij} is unimodal; but if the seismicity is clustered, the distribution of η_{ij} is bimodal. Thus, fitting the distribution of η_{ij} with a 2-component 1-D Gaussian mixture model and estimating the boundary between the two modes by the maximum likelihood method, a threshold η_0 can be found, and the background seismicity can be discerned from the clustered one, whose events have distance η_{ij} larger or smaller than the threshold η_0 , respectively [34].

Figure 4 shows the time-varying Shannon entropy of the interevent times for the declustered seismicity and the water-level fluctuations.

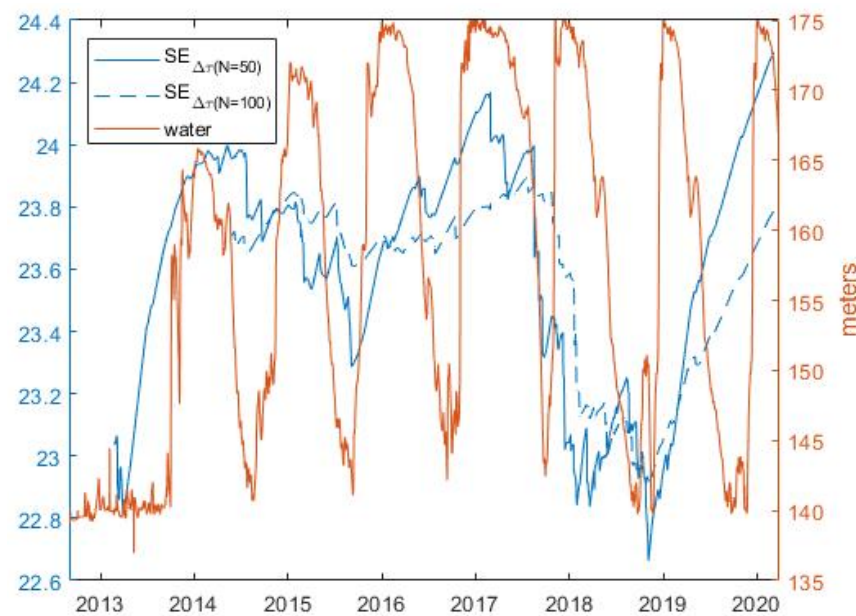


Figure 4. SE of $\Delta\tau$ for the de-clustered seismic catalogue (blue) and water level (red). Two different lengths of moving windows have been selected for calculating SE: $N = 50$ (solid) and $N = 100$ (dashed).

The SE of the seismic interevent time series of the de-clustered seismicity is characterized by a roughly similar behavior as the whole seismicity, and this suggests that the obtained results are nearly robust against the presence of seismic clusters.

5. Discussion

To assess the role of the water level as the forcing (or one of the forcings) of the time dynamics of a seismic process, it is necessary to reveal the reservoir-triggered feature in the seismicity by identifying the link between some characteristics of seismicity and water-level fluctuations. Since the water level of a reservoir generally undergoes annual cycles due to the filling and un-filling phases of the dam, a yearly oscillatory behavior in seismicity that is triggered by the reservoir might also be visible. Methods like the power spectrum of the monthly earthquake counts, the singular spectrum analysis of the monthly number of events, the Allan factor of the seismic point process, or the Schuster's spectrum of the earthquake sequence ([32] and reference therein) have been used to identify annual or quasi-annual periodicities in the time distribution of earthquakes, matching those revealed in the temporal variation in the water level, and thus allowing assessment of the existence of a dynamical link between the seismic and hydrologic processes.

The seismic area analyzed in the present study is located in the vicinity of the Song Tranh 2 hydropower plant in Vietnam. The seismic rate of the area increased after the

initial impoundment of the reservoir, and the seismic activity is still continuing, suggesting that the loading/unloading operations of the dam could be one of the sources of the occurring earthquakes.

To assess the link between the fluctuations of the water level of the reservoir and the seismic activity of the area, we analyzed the interevent times between consecutive earthquakes that represent the transitions from one earthquake to the next in the time domain.

To date, Shannon entropy has never been employed to analyze reservoir-triggered seismicity. In this paper, time-varying SE was suitable to reveal dynamical patterns in the investigated seismic series that could be correlated with the water level variability. In fact, the time-varying SE showed a quasi-periodic behavior, mimicking the oscillatory behavior of the water level. Moreover, the peaks of each cycle of the SE are mostly reached within the cycles of the water level.

The behavior of the time-varying SE suggests that the reservoir-triggered seismic process at Song Tranh 2 reservoir is characterized by alternating phases of higher disorder and lower disorder. This alternating behavior is visible in the whole seismicity as well as the de-clustered seismicity. However, the SE of the seismic series for the whole seismicity apparently behaves in a much noisier manner than that of the de-clustered seismicity; such larger irregularity in the whole seismic catalogue can be due to the presence of seismic swarms or aftershock sequences, whose time dynamics are characterized by timescales lower than those of the background seismicity, thus causing the time variation in the SE to appear more irregular.

Focusing on the time varying SE of the interevent times of de-clustered seismicity (Figure 4), the increasing phases of the SE nearly correspond to the loading or filling phases of the dam. The increase in the level of the water (corresponding to the increase in the volume of the water in the reservoir) might change the stress state of the area, causing the seismic system to be in a situation of greater disorder and instability that would lead to the increase in the rate of earthquake occurrence. Figure 5 shows, indeed, the synoptic variation in the water level and the number of events per 10 days in the Song Tranh 2 area; we see that most of the cycles of water level are followed by peaks of seismic activity culminating in relatively large earthquakes (indicated by the black dots). The increased seismic activity is the fingerprint of an increased instability in the seismic system, well depicted by the behavior of the SE of $\Delta\tau$.

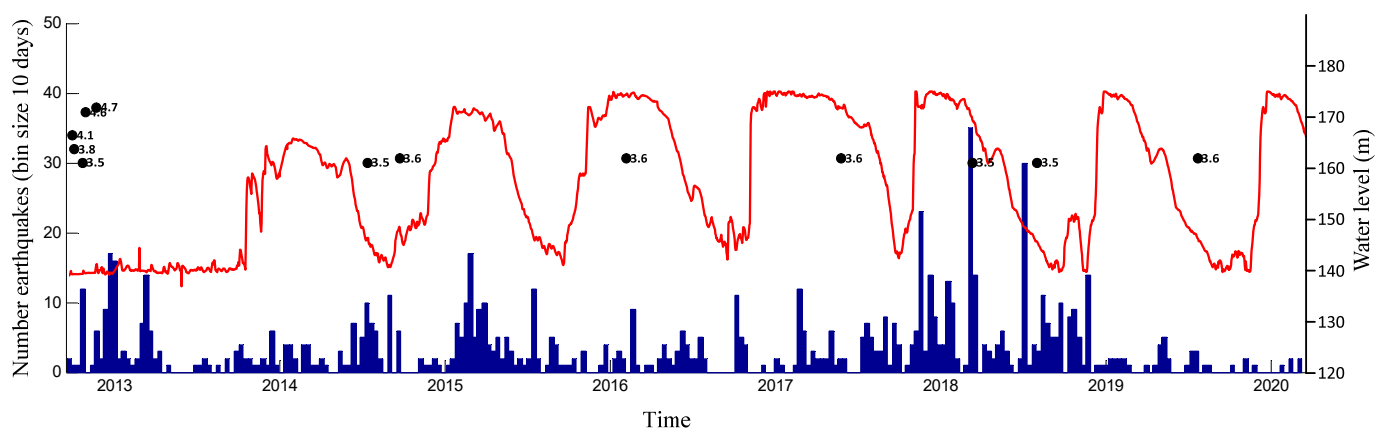


Figure 5. Temporal variation in water level in the ST2 reservoir (red) and number of earthquakes ($ML \geq 1.7$) per 10 days (blue) in the period of September 2012 to March 2020. Black dots show the time occurrence of earthquakes ($ML \geq 3.5$).

Another interesting feature of the time-varying SE of the $\Delta\tau$ is the increasing trend between approximately the second and fourth cycles of the water level; such increase corresponds to the increase in the maximum of the water level between the same cycles.

It is well known that one of the factors contributing to continued reservoir-triggered seismicity is the exceedance of reservoir levels over the previous maxima [38]; in our case, we observe that from the second to the fourth cycle the maximum of the water level in one cycle exceeds that in the previous cycle, and this seems to be well reflected in the increase in the SE, which indicates an increase in the instability and level of disorder in the seismic system. Although the number of events does not show very clearly an increase in seismic activity between the second and fourth cycles of the water level (Figure 5), it is striking that, on the contrary, the SE evidences the increase in the level of disorder and, then, in the instability in the seismic system, which underwent an increase in the stress state due to the maximum of the water level exceeding that in the previous cycle. This might have led to the greater number of events that occurred during the fifth cycle of the water level, during which the SE decreased, indicating the tendency of the seismic system toward a more stable state after the earthquakes have relaxed their energy.

Furthermore, comparing the time-varying SE of $\Delta\tau$ of the whole with that of the declustered seismicity, the range in the variation in the SE of the last one is larger than that of the first; as observed by Vogel et al. [33] the aftershocks and swarms present in the whole seismicity are characterized by successions of low and medium intensity earthquakes at short intervals producing low values of Shannon entropy. It is also probable that, since the time distribution of the de-clustered seismicity is less heterogeneous than that of the whole seismicity (seismic swarms and aftershocks being a source of heterogeneity and time clustering), the Shannon entropy is larger.

6. Conclusions

SE, well known in informational theory for its capability to characterize complex time series, has been applied to reservoir-triggered seismicity at the Song Tranh 2 reservoir in Vietnam. Our findings suggest a clear link between the time variability of the water level and the time variation in the SE of the interevent times of earthquakes. Although the potential of water reservoirs to trigger earthquakes in tectonic areas is well known, no entropic analysis of reservoir-triggered seismicity has been performed to date. Furthermore, the application of SE has furnished a novel way to interpret the occurrence of reservoir-triggered seismicity in terms of increased instability or disorder in the seismic system due to variation in water level, leading to an increase in seismic activity. Further studies will be necessary, focused on the analysis not only of several other cases of reservoir-triggered seismicity but also of other seismological variables (like epicenter distance or magnitude) in order to get a more complete description of the entropic properties of this type of seismicity and illuminate water-related causative mechanisms that are not exhaustively clarified yet. Thus, the present study suggests a new perspective for investigation of reservoir-triggered seismicity.

Author Contributions: Conceptualization, L.T.; methodology, L.T.; software, M.L.; formal analysis, L.T. and A.T.T.; investigation, L.T., A.T.T., D.T.C. and L.M.N.; resources, L.T. and A.T.T.; data curation, A.T.T., D.T.C. and L.M.N.; writing—original draft preparation, L.T.; writing—review and editing, L.T. and A.T.T.; visualization, L.T. and A.T.T.; project administration, L.T. and A.T.T.; funding acquisition, L.T. and A.T.T. All authors have read and agreed to the published version of the manuscript.

Funding: This study was funded by the Vietnam National Foundation for Science and Technology Development (NAFOSTED) under grant number 105.05-2019.328 and by CNR-VAST Italy–Vietnam common project 2020–2023, grant number QTIT01.02/20-21.

Data Availability Statement: Not applicable.

Conflicts of Interest: The authors declare no conflict of interest.

References

1. Rajendran, K.; Harish, C.M. Mechanism of triggered seismicity at Koyna: An assessment based on relocated earthquake during 1983–1993. *Curr. Sci.* **2000**, *79*, 358–363.
2. Nascimento do, A.F.; Cowie, P.A.; Lunn, R.J.; Pearce, R.G. Spatio-temporal evolution of induced seismicity at Acu reservoir, NE Brazil. *Geophys. J. Int.* **2004**, *158*, 1041–1052. [[CrossRef](#)]
3. Gupta, H.; Shashidhar, D.; Pereira, M.; Purnachandra Rao, N.; Kousalya, M.; Satyanarayana, H.V.S.; Saha, S.; Babu Naik, R.T.; Dimri, V.P. A new zone of seismic activity at Koyna, India. *J. Geol. Soc. India* **2007**, *69*, 1136–1137.
4. Gupta, H.K.; Rao, N.P.; Roy, S.; Arora, K.; Tiwari, V.M.; Patro, P.K.; Satyanarayana, H.V.S.; Shashidhar, D.; Mallika, K.; Akkiraju, V.V. Investigations related to scientific deep drilling to study reservoir triggered earthquakes at Koyna, India. *Int. J. Earth Sci. Geol. Rundsch.* **2015**, *10*, 1511–1522. [[CrossRef](#)]
5. Mikhailov, V.O.; Arora, K.; Ponomarev, A.V.; Srinagesh, D.; Smirnov, V.B.; Chadha, R.K. Reservoir induced seismicity in the Koyna–Warna region, India: Overview of the recent results and hypotheses. *Izv. Phys. Solid Earth* **2017**, *53*, 518–529. [[CrossRef](#)]
6. Valoroso, L.; Improta, L.; Chiaraluca, L.; Di Stefano, R.; Ferranti, L.; Govoni, A.; Chiarabba, C. Active faults and induced seismicity in the Val d’Agri area (Southern Apennines, Italy). *Geophys. J. Int.* **2009**, *178*, 488–502. [[CrossRef](#)]
7. Braun, T.; Cesca, S.; Kühn, D.; Martirosian-Janssen, A.; Dahm, T. Anthropogenic seismicity in Italy and its relation to tectonics: State of the art and perspectives. *Anthropocene* **2018**, *21*, 80–94. [[CrossRef](#)]
8. Reoloffs, E.A. Fault stability changes induced beneath a reservoir with cyclic variations in water level. *J. Geophys. Res.* **1988**, *93*, 2107–2124. [[CrossRef](#)]
9. Ellsworth, W. Injection-Induced Earthquakes. *Science* **2013**, *341*, 1225942. [[CrossRef](#)] [[PubMed](#)]
10. Grigoli, F.; Cesca, S.; Priolo, E.; Rinaldi, A.P.; Clinton, J.F.; Stabile, T.A.; Dost, B.; Fernandez, M.G.; Wiemer, S.; Dahm, T. Current challenges in monitoring, discrimination, and management of induced seismicity related to underground industrial activities: A European perspective. *Rev. Geophys.* **2017**, *55*, 310–340. [[CrossRef](#)]
11. Rajendran, K.; Harish, C.M.; Kumaraswamy, S.V. *Re-Evaluation of Earthquake Data from Koyna–Warna Region: Phase I*; Report to the Department of Science and Technology; Department of Science and Technology: Trivandrum, India, 1996.
12. Malik, L.K. *Damage Risk Factors for Hydraulic Engineering Structures. Safety Problems*; Nauka: Moscow, Russia, 2005.
13. Guignard, F.; Laib, M.; Amato, F.; Kanevski, M. Advanced Analysis of Temporal Data Using Fisher-Shannon Information: Theoretical Development and Application in Geosciences. *Front. Earth Sci.* **2020**, *8*, 255. [[CrossRef](#)]
14. Tang, C. Numerical simulation of progressive rock failure and associated seismicity. *Int. J. Rock Mech. Min. Sci.* **1997**, *34*, 249–261. [[CrossRef](#)]
15. Guarino, A.; Garcimartin, A.; Ciliberto, S. An experimental test of the critical behaviour of fracture precursors. *Eur. Phys. B* **1998**, *6*, 13–24. [[CrossRef](#)]
16. Lu, C.; Mai, Y.W.; Xie, H. A sudden drop of fractal dimension: A likely precursor of catastrophic failure in disordered media. *Philos. Mag. Lett.* **2005**, *85*, 33–40. [[CrossRef](#)]
17. Chelidze, T.; Kolesnikov, Y.; Matcharavili, T. Seismological criticality concept and percolation model of fracture. *Geophys. J. Int.* **2006**, *164*, 125–136. [[CrossRef](#)]
18. Rundle, J.B.; Giguere, A.; Turcotte, D.L.; Crutchfield, J.P.; Donnellan, A. Global seismic nowcasting with Shannon information entropy. *Earth Space Sci.* **2019**, *6*, 191–197. [[CrossRef](#)] [[PubMed](#)]
19. Taponnier, P.; Peltzer, G.; Armijo, R.; Coward, M.P.; Ries, A.C. On the mechanics of the collision between India and Asia. *Collision Tectonics. Geol. Soc. Spec. Publ.* **1986**, *19*, 113–157. [[CrossRef](#)]
20. Fyhn, M.B.W.; Boldreel, L.O.; Nielsen, L.H. Geological development of the Central and South Vietnamese margin: Implications for the establishment of the South China Sea, Indochinese escape tectonics and Cenozoic volcanism. *Tectonophysics* **2009**, *478*, 184–214. [[CrossRef](#)]
21. Nam, T.N. The geology of Vietnam: A brief summary and problems. *Geosci. Rep. Shizuoka Univ.* **1995**, *22*, 1–10.
22. Hoai, L.T.T.; Vuong, N.V.; Dong, B.V. Fault and Faulting Characteristics in Relationship with Reservoir Triggered Earthquakes in the Song Tranh 2 Hydropower Plan, Bac Tra My, district, Quang Nam province. *NU Hanoi J. Sci. Nat. Sci. Technol.* **2014**, *30*, 21–32, (In Vietnamese, abstract in English).
23. Hoai, L.T.T.; Vu, P.N.H.; Nguyen, N.D.; Thao, H.T.P.; Vuong, N.V. Tectonic Stress Distribution in the Song Tranh 2 Hydropower Reservoir: Implication for Induced Earthquake. *VNU J. Sci. Earth Environ. Sci.* **2021**, *37*, 24–34. [[CrossRef](#)]
24. Thai, A.T.; Purnachandra Rao, N.; Gahalaut, K.; Cao, D.T.; Le, V.D.; Cao, C.; Mallika, K. Evidence that earthquakes have been triggered by reservoir in the Song Tranh 2 region, Vietnam. *J. Seismol.* **2017**, *21*, 1131–1143.
25. Frieden, B.R. Fisher Information, Disorder, and the Equilibrium Distributions of Physics. *Phys. Rev. A* **1990**, *41*, 4265–4276. [[CrossRef](#)]
26. Shannon, C. A Mathematical Theory of Communication. *Bell Syst. Tech. J.* **1948**, *27*, 379–423. [[CrossRef](#)]
27. Telesca, L.; Lovallo, M. On the Performance of Fisher Information Measure and Shannon Entropy Estimators. *Phys. Stat. Mech. Its Appl.* **2017**, *484*, 569–576. [[CrossRef](#)]
28. Devroye, L. *A Course in Density Estimation*; Birkhauser Boston Inc.: Boston, MA, USA, 1987.
29. Janicki, A.; Weron, A. *Simulation and Chaotic Behavior of Alpha-Stable Stochastic Processes*; CRC Press: Boca Raton, FL, USA, 1993; Volume 178.

30. Troudi, M.; Alimi, A.M.; Saoudi, S. Analytical Plug-in Method for Kernel Density Estimator Applied to Genetic Neutrality Study. *EURASIP J. Adv. Signal Process.* **2008**, *2008*, 739082. [[CrossRef](#)]
31. Raykar, V.C.; Duraiswami, R. Fast optimal bandwidth selection for kernel density estimation. In Proceedings of the 2006 SIAM International Conference on Data Mining (SDM), Bethesda, MD, USA, 20–22 April 2006; pp. 524–528.
32. Telesca, L.; Thai, A.T.; Cao, D.T.; Ha, T.G. Spectral evidence for reservoir triggered seismicity at Song Tranh 2 Reservoir (Vietnam). *Pure Appl. Geophys.* **2021**, *178*, 3817–3828. [[CrossRef](#)]
33. Vogel, E.E.; Brevis, F.G.; Pastén, D.; Muñoz, V.; Miranda, R.A.; Chian, A.C.-L. Measuring the seismic risk along the Nazca–South American subduction front: Shannon entropy and mutability. *Nat. Hazards Earth Syst. Sci.* **2020**, *20*, 2943–2960. [[CrossRef](#)]
34. Zaliapin, I.; Gabrielov, A.; Wong, H.; Keilis-Borok, V.I. Clustering analysis of seismicity and aftershock identification. *Phys. Rev. Lett.* **2008**, *101*, 018501. [[CrossRef](#)] [[PubMed](#)]
35. Baiesi, M.; Paczuski, M. Scale-free networks of earthquakes and aftershocks. *Phys. Rev. E.* **2004**, *69*, 066106. [[CrossRef](#)] [[PubMed](#)]
36. Zaliapin, I.; Ben-Zion, Y. Earthquake clusters in southern California, I: Identification and stability. *J. Geophys. Res.* **2013**, *118*, 2847–2864. [[CrossRef](#)]
37. Zaliapin, I.; Ben-Zion, Y. Earthquake declustering using the nearest-neighbor approach in space-time-magnitude domain. *J. Geophys. Res. Solid Earth* **2020**, *125*, e53991. [[CrossRef](#)]
38. Durá-Gómez, I.; Talwani, P. Hydromechanics of the Koyna–Warna Region, India. *Pure Appl. Geophys.* **2010**, *167*, 183–213. [[CrossRef](#)]